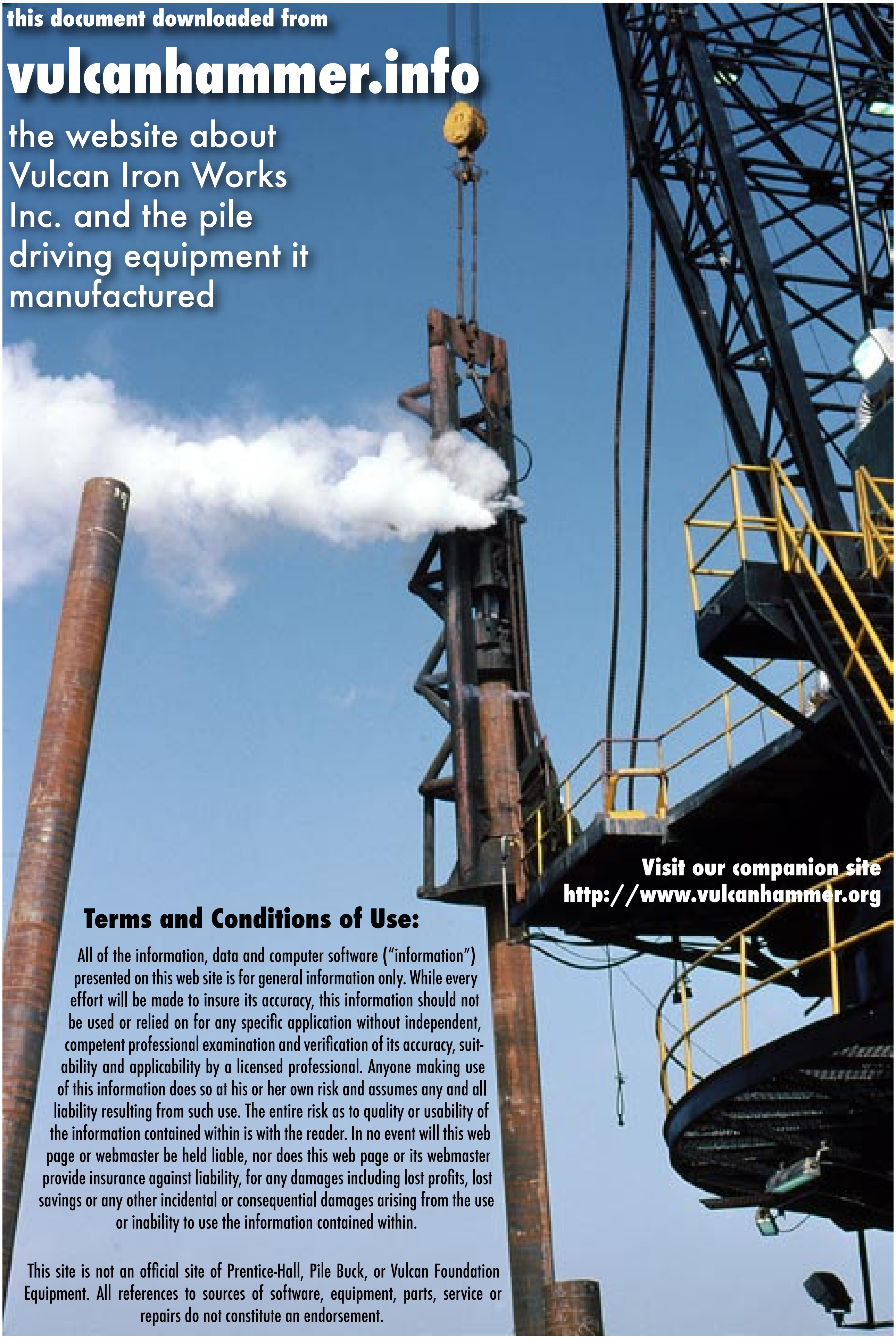

N.R. VII. [illegible]
(713) 845-1940
(713) 693-2669

2-D (AXISYMMETRY)

THREE-DIMENSIONAL ANALYSIS OF PILE DRIVABILITY

I.M. Smith, University of Manchester, England
Y.K. Chow, Fugro Ltd., Hemel Hempstead, England

SUMMARY

Pile drivability is usually assessed, in the offshore industry as well as elsewhere, on the basis of calculations which solve the one-dimensional wave equation. Clearly this is an approximation to the real situation, in which the driving process induces stress waves in the soil surrounding the pile. This paper examines the validity of the one-dimensional approximation, by comparing it with a three-dimensional (axisymmetric) one. Both one- and three-dimensional idealisations are of the finite element type.

In addition to the long-established use of wave equation predictions for drivability, recent advances in pile instrumentation during driving have led to the use of the one-dimensional equation as a means of analysing driving records with a view to predicting static capacity. In this sort of calculation, a few passages of the stress wave along the pile are analysed. In this paper, one-dimensional and three-dimensional models are compared in this context also.

Finally, offshore piles are usually driven as open-ended hollow pipes and controversy exists as to how to treat the soil "plug" in one-dimensional analyses. The ability of the three-dimensional analyses to shed light on this problem is briefly discussed.

THE ONE-DIMENSIONAL WAVE EQUATION

The classical numerical solution of this equation, proposed thirty or more years ago by E.A.L. Smith[1], still forms the basis of modern computer programs. The discretisation of pile and soil is illustrated in Figure 1 (right) and is based on a finite difference approximation to the governing differential equation. The mass and stiffness of the system are traditionally discretised as shown, the mass of the pile

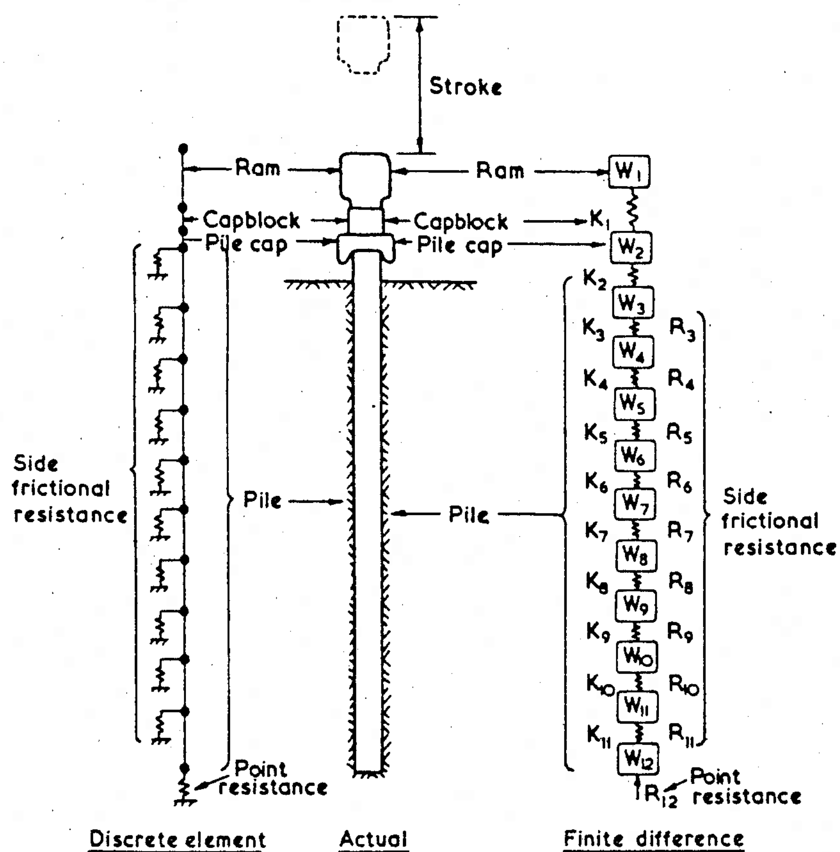

Fig.1 Method of Representing Pile

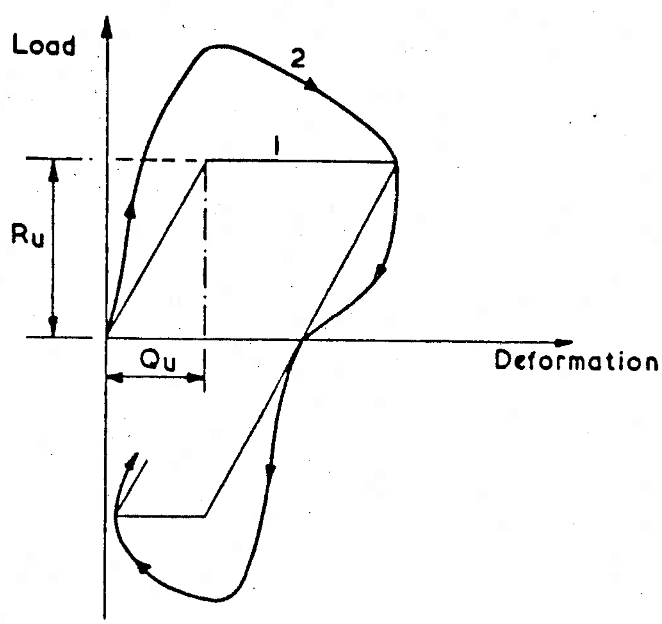

Fig.2 Load-Deformation Soil Spring

being "lumped" and the mass of the soil surrounding the pile ignored. That is, no attempt is made, as in the analysis of machine foundation vibrations for example, to consider any soil to act as an "added" mass to the vibrating system. An exception to this rule, suggested by Hereema and de Jong[2] for the driving of open-ended pipe piles offshore, involves the addition of masses and springs to represent a soil "plug" inside the hollow pile.

The soil resistance, R, is traditionally assumed to be elasto-viscoplastic as illustrated in Figure 2. The ultimate static capacity, R_u, of each soil "spring" is estimated independently and the elastic displacement or quake, Q_u, is still often taken to be the 2.54mm (0.1 inch) originally recommended by E.A.L. Smith. Thus in the absence of viscosity, a soil spring would traverse load path 1 in Figure 2.

In order to obtain a better fit with field data, soil springs are actually assumed to follow something like path 2 in Figure 2. The added resistance is ascribed to velocity-dependent viscous effects but may actually be an attempt to cater for some radiation damping as well, as will be discussed later. At any rate, various viscous models have been proposed, in which the viscous resistance is proportional to velocity of penetration, static resistance, pile impedance, velocity of penetration to the power 0.2 and so on. These various viscous models are not the concern of the present paper. Table 1 shows some typical soil data used in offshore studies, and what becomes immediately apparent is the need in the calculations for the non-standard soil mechanics parameters Q_u, J_s and J_p, the elastic quake, shaft damping and point damping respectively.

Figure 1 (left) shows a slightly different one-dimensional pile discretisation. This is based on a one-dimensional finite element model of the pile which permits the pile's mass either to be "lumped" as in the finite difference case, or continuously distributed along the element as it must be in reality. However, despite minor variations (for example the capblock is usually assumed to be massless in the traditional programs) the finite element and finite difference idealisations should give essentially the same results for the same physical assumptions. The authors prefer the finite element model for personal reasons of program adaptability, eg. Smith[3].

Author	Field	Soil Type	Quake (mm) Side	Quake (mm) Tip	Damping (s/m) J_s	Damping (s/m) J_p
1. Naughton & Miller (1978)	Hondo Platform	Stiff OC clay	2.54	2.54	0.164	0.492
2. Young et al (1978)	Thistle Platform	Stiff OC clay	2.54	0.51 12.70	0.49	0.16 0.49
3. Sutton et al (1979)	Forties Platform	Lightly OC clays with layers of dense sand	2.54	2.54	0.656	0.033
4. Sullivan & Ehlers (1972)	(a) Gulf of Mexico (b) Off Louisiana coast (c) Off coast of Nigeria	V. soft to stiff clay Soft to firm clay Firm to v. stiff clay	2.54	2.54	0.492	0.492

TABLE 1 Parameters Used in Offshore Drivability Predictions

ALGORITHM SENSITIVITY

All numerical solutions of differential equations are approximate, the only question being the magnitudes of the errors committed. Figures 3 and 4 illustrate one aspect of algorithm sensitivity. Three well known algorithms were used to solve a one-dimensional problem (based on

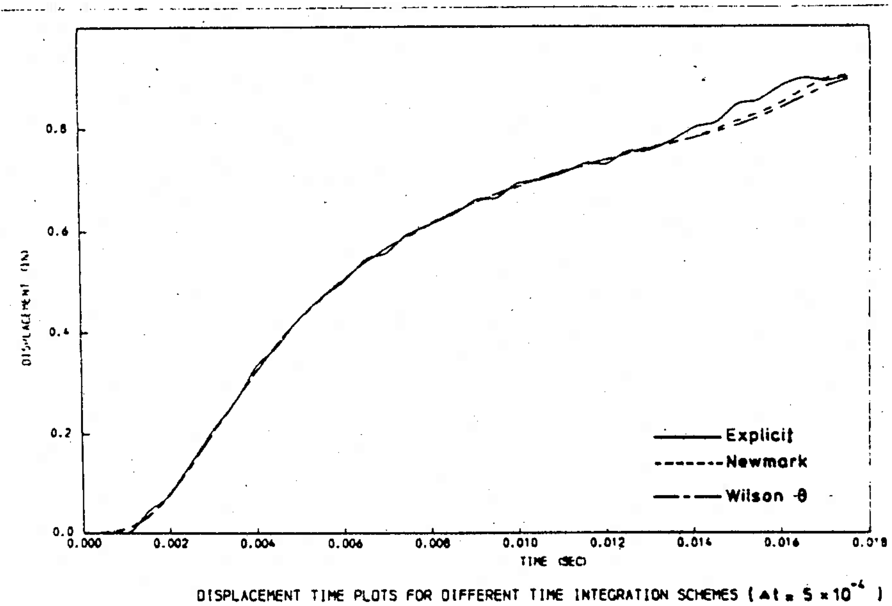

Fig.3 Displacement-Time for Different Integration Schemes ($\Delta t = 5 \times 10^{-4}$)

the original example chosen by Smith[1]) with a fixed timestep. The algorithms were the conventional explicit method, a central difference implicit method labelled "Newmark" and a second implicit method popular in structural dynamics and labelled "Wilson". Figure 3 shows that the displacement of the pile tip, the parameter traditionally of interest in these computations, is insensitive to algorithm choice. However, the accelerations in the pile, see Figure 4, are quite different for the three different methods of computation.

A second aspect of algorithm sensitivity is shown in Figures 5 and 6

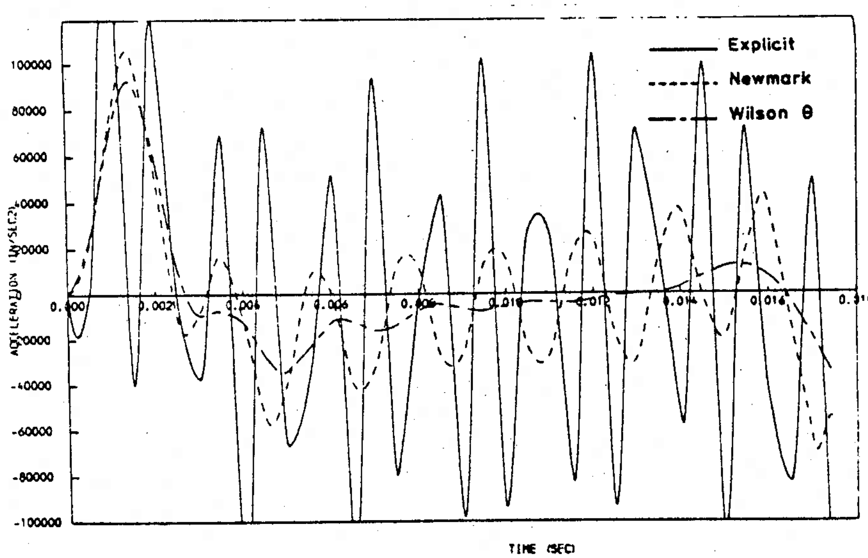

ACCELERATION TIME PLOTS FOR DIFFERENT TIME INTEGRATION SCHEMES ($\Delta t = 5\times10^{-4}$)

Fig.4 Acceleration-Time for Different Integration Schemes($\Delta t = 5 \times 10^{-4}$)

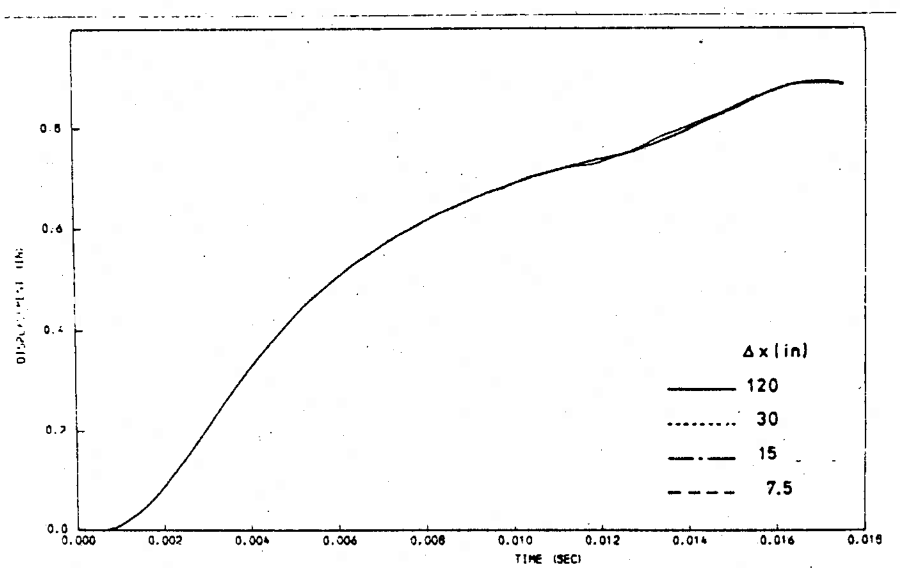

Fig.5 Displacement-Time Plots (Wilson) (Consistent Mass)

where the test problem was solved by a typical algorithm (Wilson's actually) for a fixed timestep but varying space step sizes. Again pile displacement is seen to be insensitive to space discretisation while acceleration is highly sensitive.

The consequence of these sensitivity studies is that although an algorithm may work quite well in the role for which it was originally intended, care is necessary in new applications, Smith[4]. For example, these sorts of algorithm have traditionally <u>only</u> been used to calculate the "set" or plastic displacement of the pile tip, shown above to be an insensitive parameter. Indeed a survey by Saxena[5] showed that most popular programs cease computing after the tip displacement reaches its first maximum value, and the set is inferred by subtracting the quake from that maximum. However, there is an increasing tendency to use one-dimensional calculations in conjunction with field monitoring of strains and accelerations in driven piles, eg. Goble and Rausche[6]. These computations usually need to run for a much longer time than that necessary to establish pile set, and clearly the scope for algorithmic errors is greater. Of course appropriate reductions of space and time steps should lead to a converged result, appropriate to that one-dimensional model.

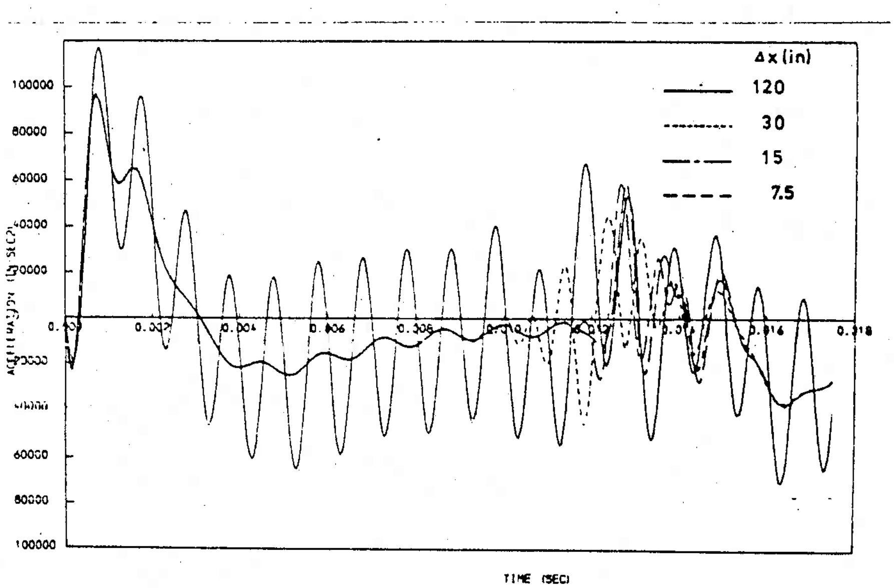

Fig.6 Acceleration-Time Plots (Wilson) (Consistent Mass)

THREE-DIMENSIONAL ANALYSIS

For piles with axial symmetry, for example the pipe piles driven offshore, it is perfectly feasible to carry out computations of drivability using a three-dimensional axisymmetric model of the pile and its surrounding soil. Numerically this could be done in various ways, but the authors again employ the finite element method, a typical model of a (solid) axisymmetric pile being shown in Figure 7. Pile and soil are represented by 8-noded elements of quadrilateral cross-section as shown and thin 6-noded interface elements separate pile and soil to allow for relative slippage.

Such a model represents much more faithfully the realities of pile driving in that stress waves are generated in the soil mass. In order that these waves are not reflected from mesh boundaries, viscous dashpots forming a "standard viscous boundary" (Lysmer and Kuhlemeyer[7]) are placed around the boundaries, Chow[8].

An advantage of this type of model is that more standard soil mechanics parameters can be used to describe the properties of the soil mass. The analyses described in this paper are restricted to piles in

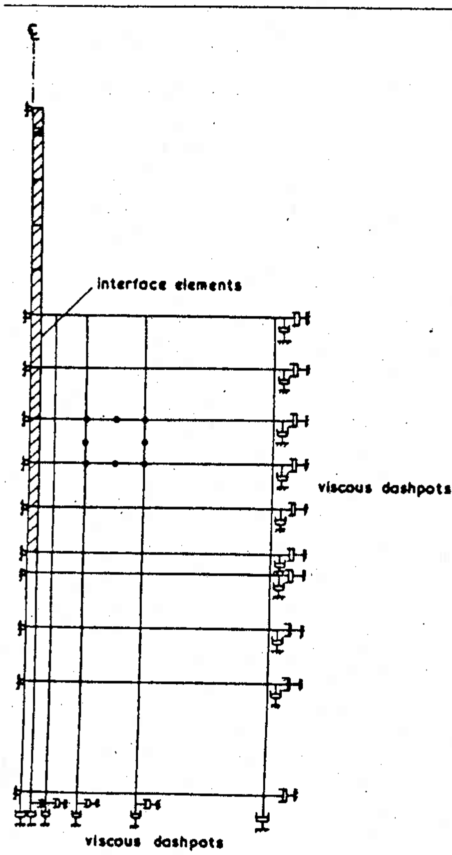

Fig.7 Finite Element Model for Pile Drivability

"clay" which is assumed to be essentially undrained during driving. The clay is idealised as elastic-perfectly plastic yielding according to the von Mises criterion, and undergoing associated (no-volume-change) flow. The elastic properties are a Young's modulus, E, and a Poisson's ratio, ν. The yield stress is a simple function of C_u, the undrained strength as measured in a triaxial or plane strain test.

Radiation damping now occurs in the model automatically, but in some analyses viscous damping has been included as well. When this is done, it applies only to the nodal points along the shaft and tip of the pile, in a manner similar to that used in the one-dimensional analyses.

To avoid any difficulties caused by plug movement, closed-ended pipe piles are considered first. For such piles the static tip resistance, N_c, in the formula $q_{ult} = C_u . N_c$, is computed to be about 9, in line with current practice. The strength of the interface elements was taken to be 0.5 C_u to take some account of remoulding during driving.

The Wilson implicit algorithm was used to integrate the three-dimensional wave equation and in some calculations, the initial conditions were taken to be a prescribed ram velocity. However, another method for offshore piles is to use the manufacturer's force-time plot for a given hammer and pile combination, and this has been used in some of the calculations also. (These initial conditions have previously led to difficulties in analysing diesel-driven piles using some standard programs). Nonlinearity is accounted for by the "initial stress" type of algorithm.

COMPARISON OF THREE-DIMENSIONAL AND ONE-DIMENSIONAL MODELS

(a) Wave propagation down a pile in the absence of soil resistance.

Case 1: End bearing pile.

A simple test case was selected for which an exact solution is known, namely a uniform rod, fixed at one end and free at the other and subjected to a constant impact force. Figure 8 shows a comparison of one-dimensional finite element solutions with the true solution for both lumped and consistent mass assumptions. The latter are clearly superior although the contrary is sometimes claimed in the literature.

The corresponding comparison for the three-dimensional finite element approximation is shown in Figure 9. Here, all the numerical solutions adopted the consistent mass idealisation and it can be seen

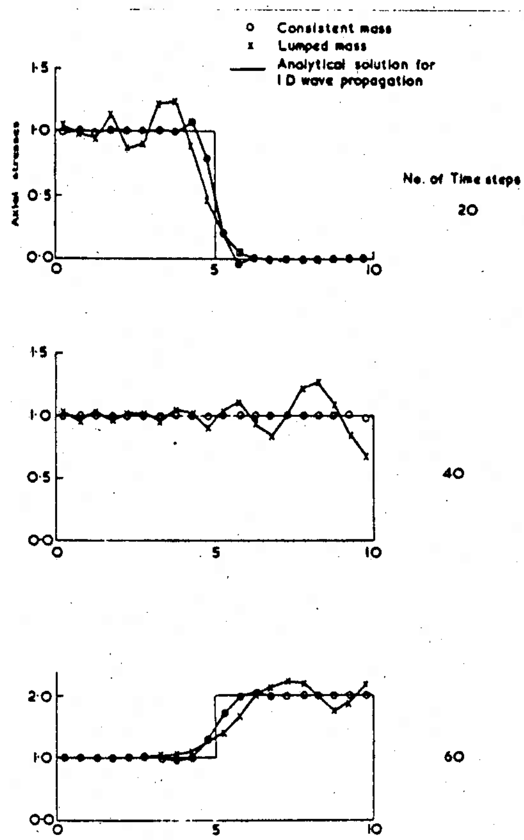

Fig.8 Axial Wave in 1-D Rod (1-D Elements)

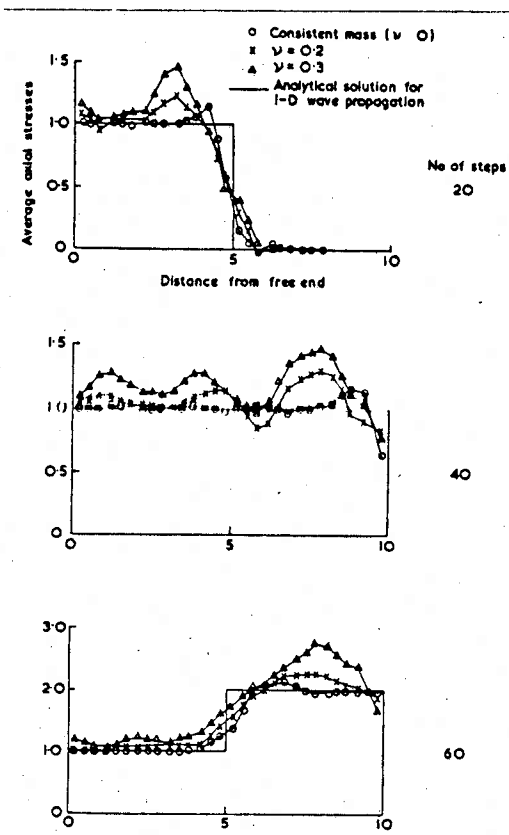

Fig.9 Axial Wave in 3-D Rod (Axisymmetric Elements)

that Poisson's ratio has a noticeable effect on stresses although not on axial displacements. However the best comparison should be when Poisson's ratio is zero and the quality of the three-dimensional numerical solutions is very similar to that of the one-dimensional ones.

Case 2: Free-free pile (no soil resistance).

The pile data are given in Table 2. The initial conditions were a prescribed hammer velocity and Figure 10 shows a comparison of the pile tip displacements.

Hammer Data	MRBS 750 Weight = 75 kN Impact Energy = 84.4 kNm
Capblock	Diameter = 0.72m Height = 0.18m
Anvil	Weight = 31.5 kN
Pile	Outer Diameter = 1.524m Wall Thickness = 63.5mm Total Length = 36m
Soil	Pile Penetration = 20m Cohesive

TABLE 2 Driving Accessories and Pile Data

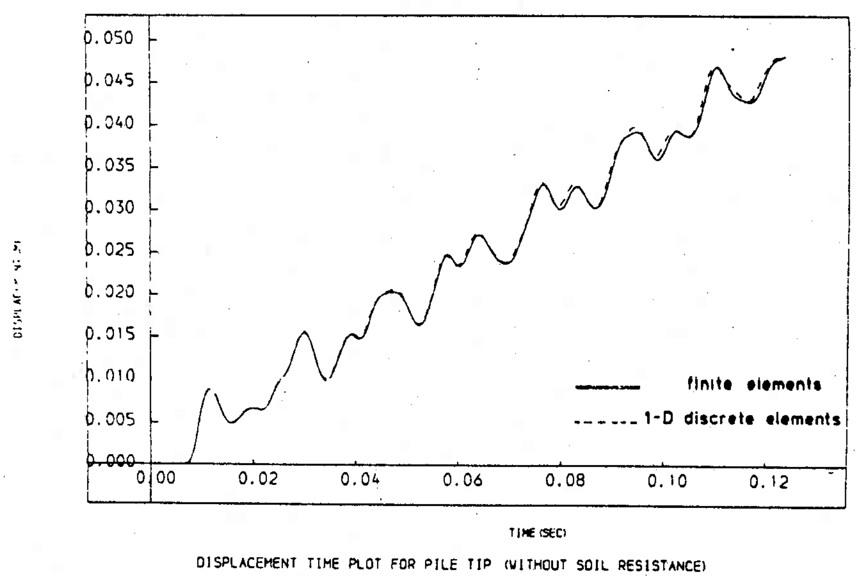

Fig.10 Displacement-Time for Pile Tip (No Soil Resistance)

The agreement is very close, and the same can be said of velocities and accelerations. In this case, Poisson's ratio had no marked effect on the three-dimensional solutions for axial displacement etc. as before.

(b) Wave propagation down a pile embedded in "clay".

The pile data are again as listed in Table 2, but the pile is now embedded to a depth of 20m in an elasto-plastic idealisation of undrained clay.

Case 1: Soil with $C_u = 100$ kN/m^2, $E = 1000\ C_u$, $\alpha = 0.5$, $\rho = 0.01$ t/m^3. No viscous damping.

This example is intended to demonstrate the difference between the one-dimensional and three-dimensional analyses due solely to the stiffness of the soil surrounding the pile. In the one-dimensional case the soil spring stiffness is defined by the traditional quake value of 2.54mm, while in the three-dimensional model the soil's mass is assigned a very low value. No viscous damping is taken into account. Figure 11 shows the comparison of the computed tip displacements. They are clearly quite similar in terms of hills and hollows but the curves are displaced relative to one another. This can be ascribed to small inertia effects in the three-dimensional model together with the differences in soil stiffness and distribution.

When the soil strength and the Poisson's ratio of the pile were varied, essentially similar results to Figure 11 were obtained.

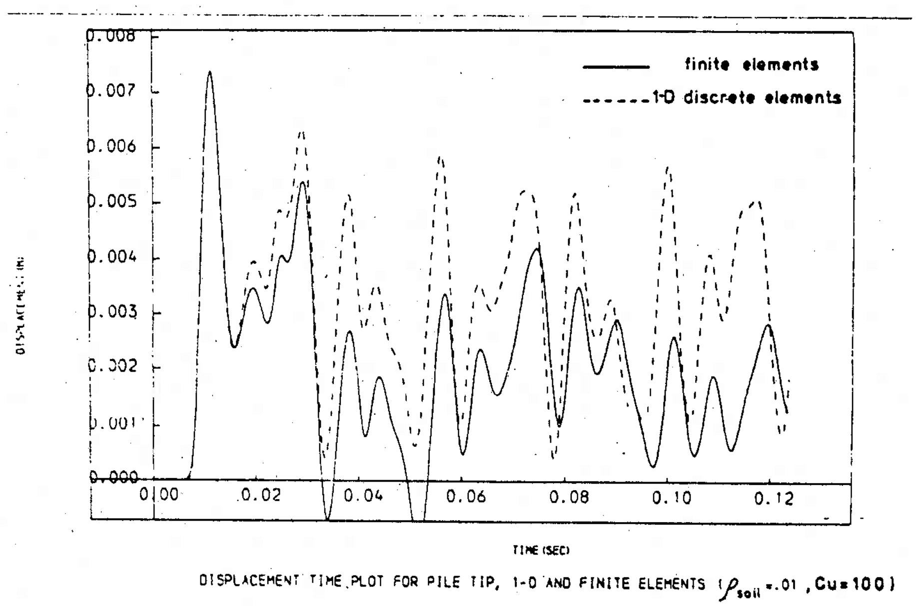

Fig.11 Displacement-Time for Pile Tip ($\rho_{soil} = 0.1$, $C_u = 100$)

Case 2: Soil with $C_u = 100$ kN/m^2, $E = 1000\ C_u$, $\alpha = 0.5$,
$\rho = 2.1$ t/m^3. No viscous damping.

In this case the influence of soil inertia was fully taken into account in the three-dimensional model. Figure 12 shows the comparison of the tip displacements which are quite close at small times after impact, but progressively diverge with time, the three-dimensional model giving the more damped response leading to an equilibrium "set" of some 4mm. The one-dimensional calculation did not achieve equilibrium although if the E.A.L. Smith suggestion of subtracting 2.54mm from the first peak displacement is used, a rather similar set of some 5mm would be predicted. Of course it could be argued that the viscous parameter J in the one-dimensional analysis is partially intended to model some radiation damping. Its inclusion reduces the one-dimensional set by about 1mm for this clay strength.

When the soil strength is raised to 500 kN/m^2, equivalent to the hardest clays encountered in the North Sea, Figure 13 shows the comparative tip displacement plots. The curves diverge even earlier for the stronger soil with the three-dimensional calculation being very strongly damped, leading to an equilibrium set of some 0.7mm. When the Smith method is applied to the one-dimensional result, a quite similar set of some 0.5mm is predicted. However, if viscous damping is now included in the one-dimensional model, a zero set would be predicted, ie. the pile could not be driven.

Results for weak clay, $C_u = 25$ kN/m^2, give the closest agreement

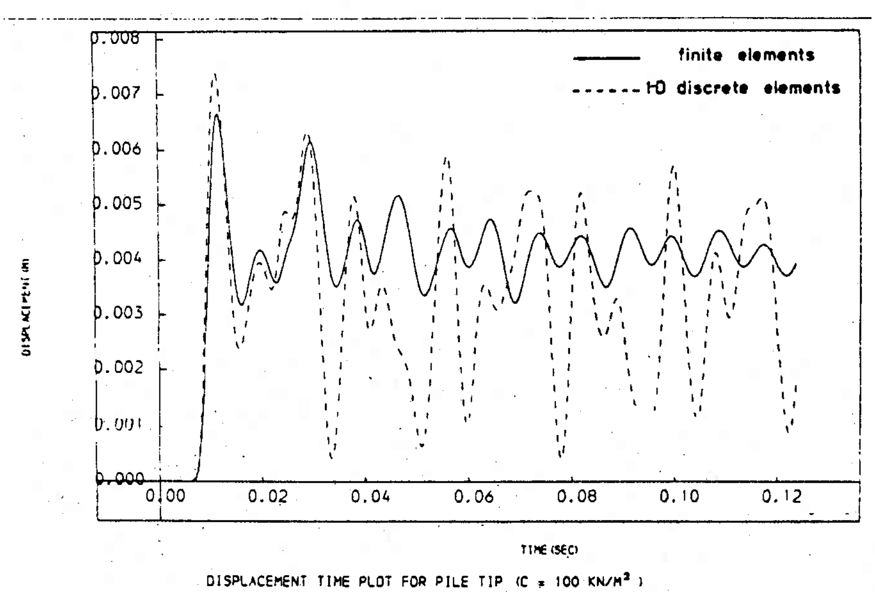

Fig.12 Displacement-Time for Pile Tip ($C_u = 100$ kN/m^2)

between one-dimensional and three-dimensional models. A noteworthy observation is that in this case the first peak on the displacement-time curve is not the maximum, which is achieved later on.

Thus from these studies it can be inferred that the one-dimensional calculation can accurately predict pile set, but that in detail the performance of the pile is not closely followed, especially for stiff soils.

Additional computations using double and treble the hammer energy led to essentially the same conclusions.

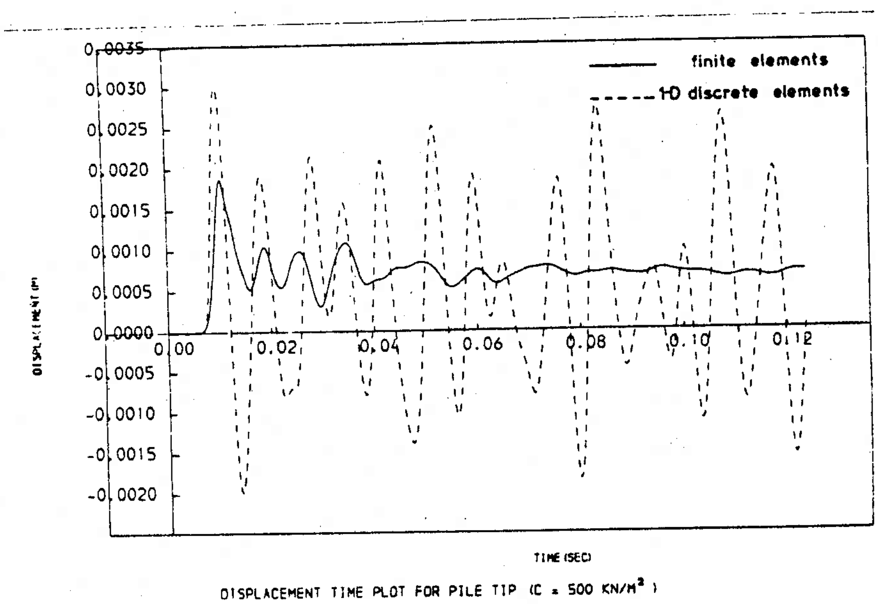

Fig.13 Displacement-Time for Pile Tip (C_u = 500 kN/m^2)

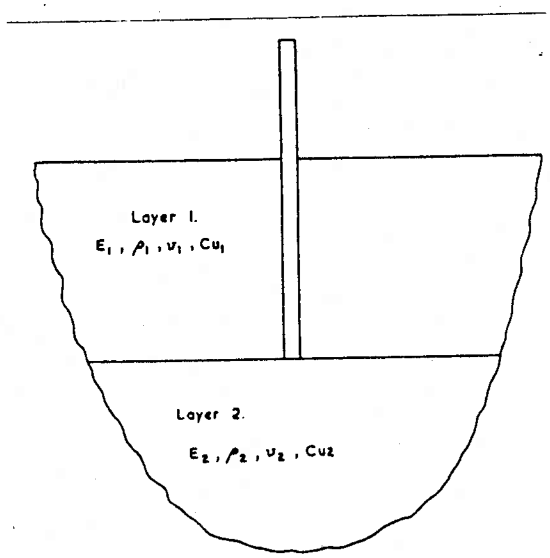

Fig.14 Pile Drivability: Two-Layer Problem

PARAMETRIC STUDIES USING THE THREE-DIMENSIONAL MODEL

The basic geometry is shown in Figure 14, the pile details being again those of Table 2. In the studies, the properties of layer 1 were kept constant while those of layer 2 were varied.

Figure 15 shows the effect of increasing the undrained strength of the clay in layer 2, keeping the other soil parameters constant. The effect is to decrease the maximum tip displacement and to increase the mobilised end resistance as one would expect.

A second point worthy of study is the influence of the clay's elastic stiffness on the results for a constant clay strength. Much evidence for stiffer clays suggests that in the equation $E = \beta C_u$, the factor β is of the order of 500 – 1000. With the undrained strength of layer 2 kept at 100 kN/m^2, β was varied from 250 to 1250. Defining the end bearing resistance factor during driving as N_D, where

$$N_D = \frac{\text{Maximum Tip Load}}{\text{Pile Tip Area x Undrained Clay Strength}}$$

it can be seen from Figure 16 that N_D is usually considerably higher than the N_c of about 9 computed and measured in static analyses and tests. For β values in the range 500 to 1000, N_D increases from about

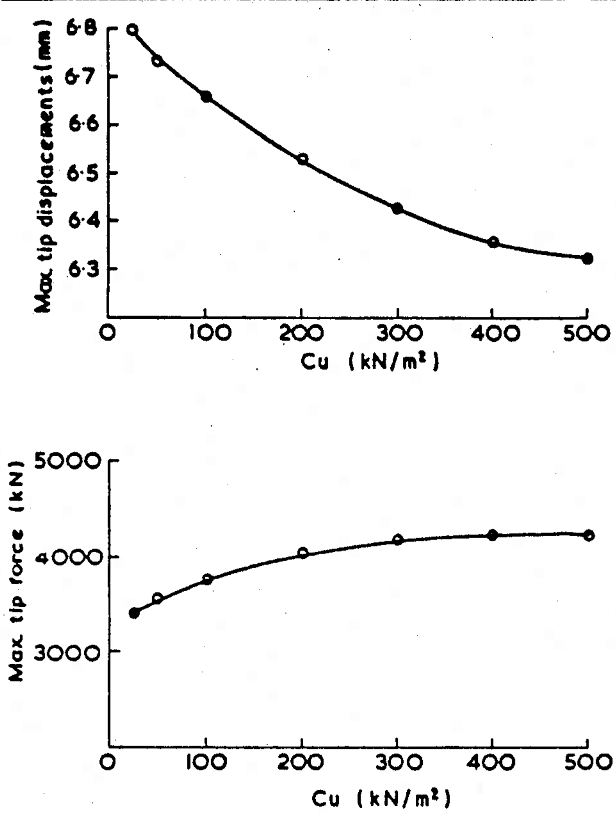

Fig.15 Variation of Maximum Tip Response with C_u (Constant E)

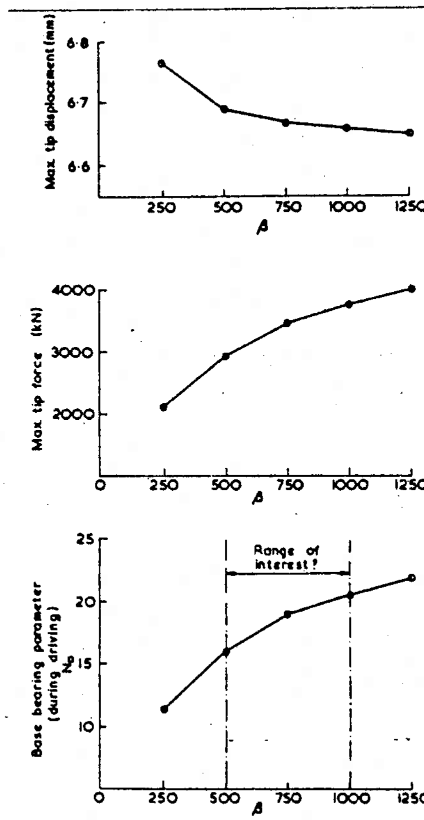

Fig.16 Sensitivity of Parameters to β ($E = \beta C_u$, Constant C_u)

16 to 20.5, and this must be attributed to inertia and radiation damping effects alone, since no clay viscosity was assumed.

Mobilisation of N_D During Driving

The above results suggest that N_D varies with C_u and with β, and Figure 17 shows further evidence. In these results C_u for layer 1 is 100 kN/m^2. The same results, for the case β = 1000, are plotted in Figure 18 in terms of mobilised tip displacement. The effect of changing C_u in layer 1 to 25 kN/m^2, other factors remaining constant, is shown in Figure 19. Somewhat higher N_D values result.

The strongest trend apparent is the decrease of N_D with increasing soil strength. Confirmation of this comes from cone penetration tests in the North Sea conducted by Fugro[9], see Figure 20. This shows N_D values as high as 30 for some weak clays, reducing to less than 10 for some of the strongest clays.

Quake Values

Figures 18 and 19 allow an estimate of the tip quake computed in the three-dimensional analyses. If this is identified roughly as the tip displacement when N_D reaches its maximum, it can be seen to be

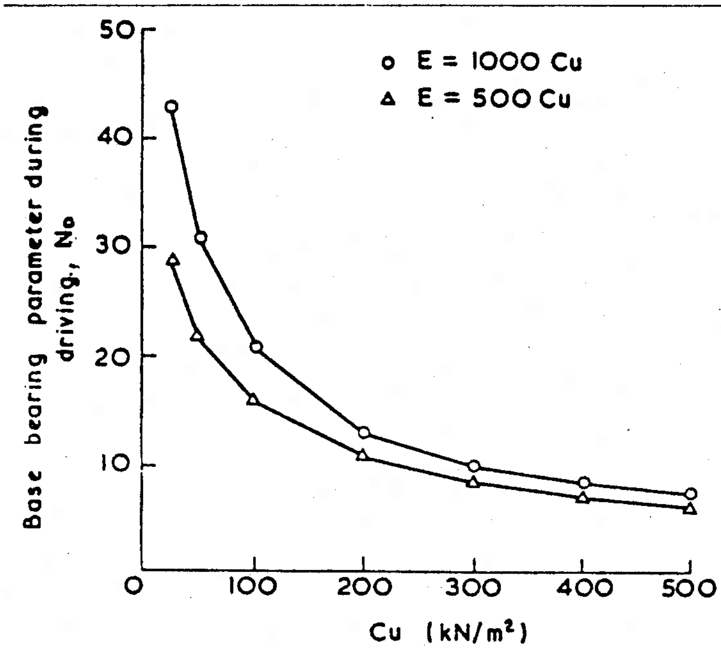

Fig.17 Variation of N_D with C_u

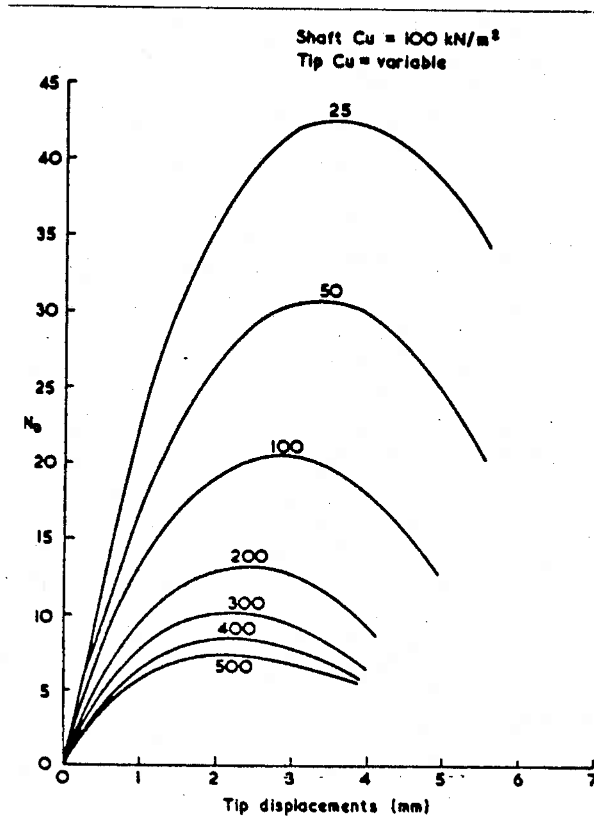

Fig.18 N_D During Driving (Closed-Ended Pile) remarkably insensitive to soil strength and elasticity. Indeed the full range is only from about 2mm to 4mm, the higher values being for the softer soils. For typical clays encountered offshore, 2.5mm is a remarkably good estimate, in agreement with E.A.L. Smith's original suggestion.

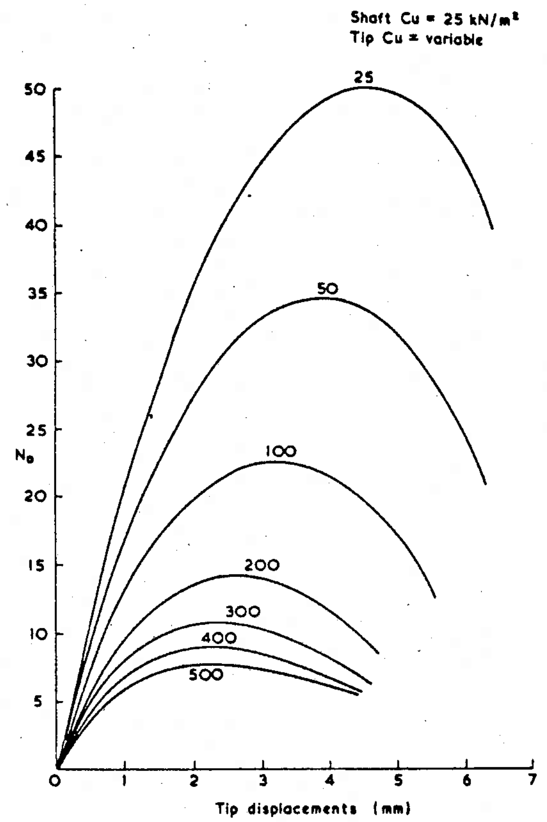

Fig.19 N_D During Driving (Closed-Ended Pile)

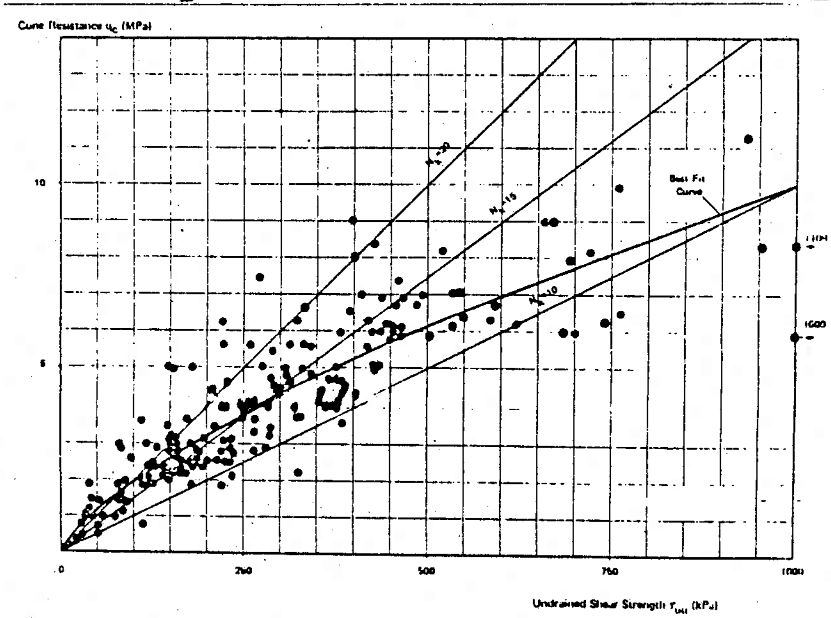

Fig.20 Variation of Cone Resistance with C_u

Estimation of shaft quake is more subjective. However Table 3 shows the mobilised maximum shaft force for a pile driven into uniform soils with varying shear strengths. If the side quake is identified with the pile head amplitude during driving, again a value remarkably close to 2.5mm is computed.

Undrained Shear Strength(kN/m^2)	Max. Mobilised Shaft Force(kN)	Proportion of Shaft Resistance	Pile Head Movement(mm)
25	1191	1.00	2.66
50	2377	0.99	2.77
100	4651	0.97	2.66
200	9237	0.96	2.63
300	13140	0.91	2.61
400	16570	0.87	2.74
500	19390	0.81	2.73

TABLE 3 Mobilised Skin Friction with Movement of Pile Head

Use of Driving Records to Estimate Static Capacity

A typical approach, eg. Gravare et al[10], predicts the total pile resistance (static capacity) according to the formula

$$R_{total} = \frac{1}{2}\text{ (Sum of pile top forces at times } t_1 \text{ and } t_2 \text{ derived from strain measurements)}$$
$$+ \frac{1}{2}\text{ (Difference of pile top forces at times } t_1 \text{ and } t_2 \text{ derived from velocity measurements).}$$

The times t_1 and t_2 are taken to be 2L/c apart, where L is the pile length and c the speed of the wave propagation. Time t_1 is that at which the pile top force first reaches a maximum. Typical results obtained using this formula for the pile described previously, embedded in clays of strength 25, 100 and 500 kN/m^2, are shown below:

C_u	25	100	500
Computed	2,500	8,500	20,000
Actual	1,607	6,430	32,148

In order to obtain these results the peak forces in the vicinity of t_2 were taken, although they occurred at different times in the two models. The agreement with static capacity is only of a general nature. Skill is therefore necessary in the prediction of pile capacities in this way.

Plugging of Pipe Piles

By modelling open-ended piles using axisymmetric finite elements, it is possible to take account of the soil plug and soil-pile interface inside a hollow pile. Lack of space precludes a detailed treatment herein, but the finite element results show that the plug behaves quite differently in static and impact circumstances. In the former, skin friction is not fully mobilised on the inner wall of the pile and so the statically loaded pile behaves as "plugged". However, in the impact driving case, the inertia of the plug comes into play, and full skin friction tends to be mobilised inside the pile so that during driving the pile behaves as "unplugged". This may help to explain the observation that closed-ended piles can be easier to drive in clays than open-ended ones.

CONCLUSIONS

One-dimensional and three-dimensional models of impact driven piles have been compared. There are significant differences in behaviour, particularly for piles driven in stiffer, stronger soils.

REFERENCES

1. Smith, E.A.L. "Pile driving analysis by the wave equation," Journal of the Soil Mechanics and Foundations Division, ASCE, Vol.86, No.SM4, Aug. 1960.
2. Heerema, E.P. and de Jong, A. "An advanced wave equation computer program which simulates dynamic pile plugging through a coupled mass-spring system," Conference on Numerical Methods in Offshore Piling, Institution of Civil Engineers, London, 22-23 May 1979.
3. Smith, I.M. "Programming the finite element method," John Wiley and Sons, 1981.
4. Smith, I.M. "Transient phenomena of offshore foundations," Ch.5 in 'Numerical Methods in Offshore Engineering' (Editors: O.C. Zienkiewicz, R.W. Lewis and K.G. Stagg), John Wiley & Sons, 1978.
5. Saxena, S.K. "Wave equation for piles - an evaluation," Proc. Imp. Computer Prog. in Geotechnical Eng., Vol.1, p.223, 1981.

6. Goble, C.G. and Rausche, F. "Pile drivability predictions by CAPWAP," Conference on Numerical Methods in Offshore Piling, Institution of Civil Engineers, London, 22-23 May 1979.

7. Lysmer, J. and Kuhlemeyer, R.L. "Finite dynamic models for infinite media," Journal of Engineering Mechanics Division, ASCE, Vol.95, EM4, pp.859-877, August 1969.

8. Chow, Y.K. "Dynamic behaviour of piles," Ph.D. Thesis, University of Manchester, 1981.

9. Fugro Ltd. Private Communication, 1981.

10. Gravare, C.J., Goble, C.G., Rausche, F. and Likins, G. "Pile driving construction control by the Case method," Ground Engineering, March 1980.